

Yield criteria for quasibrittle and frictional materials

Davide Bigoni and Andrea Piccolroaz
Dipartimento di Ingegneria Meccanica e
Strutturale, Università di Trento,
Via Mesiano 77, I-38050 Trento, Italia
email: bigoni@ing.unitn.it

August 29, 2002

Abstract

A new yield/damage function is proposed for modelling the inelastic behaviour of a broad class of pressure-sensitive, frictional, ductile and brittle-cohesive materials. The yield function allows the possibility of describing a transition between the shape of a yield surface typical of a class of materials to that typical of another class of materials. This is a fundamental key to model the behaviour of materials which become cohesive during hardening (so that the shape of the yield surface evolves from that typical of a granular material to that typical of a dense material), or which decrease cohesion due to damage accumulation. The proposed yield function is shown to agree with a variety of experimental data relative to soil, concrete, rock, metallic and composite powders, metallic foams, porous metals, and polymers. The yield function represents a single, convex and smooth surface in stress space approaching as limit situations well-known criteria and the extreme limits of convexity in the deviatoric plane. The yield function is therefore a generalization of several criteria, including von Mises, Drucker-Prager, Tresca, modified Tresca, Coulomb-Mohr, modified Cam-clay, and —concerning the deviatoric section— Rankine and Ottosen. Convexity of the function is proved by developing two general propositions relating convexity of the yield surface to convexity of the corresponding function. These propositions are general and therefore may be employed to generate other convex yield functions.

Keywords: B. yield criteria; B. elastic-plastic material; B. concrete; B. foam material; B. geological material; B. granular material

1 Introduction

Yielding or damage of quasibrittle and frictional materials (a collective denomination for soil, concrete, rock, granular media, coal, cast iron, ice, porous metals, metallic foams, as well as certain types of ceramic) is complicated by many effects, including dependence on the first and third stress invariants (the so-called ‘pressure-sensitivity’ and ‘Lode-dependence’ of yielding), and represents the subject of an intense research effort. Restricting attention to the formulation of yield criteria, research moved in two directions: one was to develop such criteria on the basis of micromechanics considerations, while another was to find direct interpolations to experimental data. Examples of yield functions generated within the former approach are numerous and, as a paradigmatic case, we may mention the celebrated Gurson criterion (Gurson, 1977). The latter approach was also broadly followed, providing some very successful yield conditions, such as for instance the Ottosen criterion for concrete (Ottosen, 1977). Although very fundamental in essence, the micromechanics approach has limits however, particularly when employed for geomaterials. For instance, it is usually based on variational formulations, possible—for inelastic materials—only for solids obeying the postulate of maximum dissipation at a microscale, which is typically violated for frictional materials such as for instance soils.

A purely phenomenological point of view is assumed in the present article, wherein a new yield function¹ is formulated, tailored to interpolate experimental results for quasibrittle and frictional materials, under the assumption of isotropy. The interest in this proposal lies in the features evidenced by the criterion. These are:

- finite extent of elastic range both in tension and in compression;
- non-circular deviatoric section of the yield surface, which may approach both the upper and lower convexity limits for extreme values of material parameters;
- smoothness of the yield surface;
- possibility of stretching the yield surface to extreme shapes and related capability of interpolating a broad class of experimental data for different materials;
- reduction to known criteria in limit situations;
- convexity of the yield function (and thus of the yield surface);
- simple mathematical expression.

¹ We need not distinguish here between yield, damage and failure. Within a phenomenological approach, all these situations are based on the concept of stress range, bounded by a given hypersurface defined in stress space.

None of the above features is *essential*, in the sense that a plasticity theory can be developed without all of the above, but all are *desirable* for the development of certain models of interest, particularly in the field of geomaterials. This is a crucial point, deserving a carefully explanation. In particular, while some of the above requirements have a self-evident meaning, smoothness and convexity need some discussion.

Although experiments are inconclusive in this respect (Naghdi et al. 1958; Paul, 1968; Phillips, 1974), theoretical speculations (sometimes criticized, Naghdi and Srinivasa, 1994) suggest that corners should be expected to form in the yield surface for single crystals and polycrystals (Hill, 1967). Therefore, smoothness of the yield surface might be considered a mere simplification in the constitutive modelling of metals. However, the situation of quasibrittle and frictional materials is completely different. For such materials, in fact, evidence supporting corner formation is weak², so that, presently, smoothness of the yield surface is a broadly employed concept and models developed under this assumption are still very promising. Moreover, corners often are included in the constitutive description of a material for the mere fact that an appropriate, smooth yield function is simply not available (this is usually the case of the apex of the Drucker-Prager yield surface and of the corner which may exist at the intersection of a smooth, open yield surface with a cap).

Regarding convexity of the yield surface, we note that this follows for polycrystals from Schmid laws of single crystals (Bishop and Hill, 1951; Mandel, 1966). However, differently from smoothness, convexity is supported by experiments in practically all materials and is a useful mathematical property, which is the basis of limit analysis and becomes of fundamental importance in setting variational inequalities for plasticity (Duvaut and Lions, 1976). We may therefore conclude that—in the absence of a clear and specific motivation—it is not sensible to employ a yield function that violates convexity.

A number of failure surfaces have been proposed meeting some of the above requirements, among others, we quote the Willam and Warnke (1975), Ottosen (1977) and Hsieh et al. (1982) criteria for concrete, the Argyris et al. (1974), Matsuoka and Nakai (1977), Lade and Kim (1995), and Lade (1997) criteria for soils. For all these criteria, while some information can be found about the range of parameters corresponding to convexity of the yield *surfaces*, nothing is known about the convexity of the corresponding yield *functions*.

Convexity of a yield function implies convexity of the corresponding yield surface, but convexity of a level set of a function does not imply convexity of the function itself. While it can be pointed out that a convex yield function can *in principle* always be found to represent a convex yield surface, the ‘practical problem’ of finding it in a reasonably simple form may be a formidable one. From this respect, general propositions would be of interest, but the only contribution of which the authors are aware in this respect is quite recent (Mollica and Srinivasa, 2002). A purpose of the present paper is to pro-

²Some argument in favour of corner formation in geomaterials have been given by Rudnicki and Rice (1975).

vide definitive results in this direction. In particular, the range of material parameters corresponding to convexity of the yield function proposed in this paper is obtained by developing a general proposition that can be useful for analyzing convexity of a broad class of yield functions. The proposition is finally extended to introduce the possibility of describing a modification in shape of the deviatoric section with pressure. The propositions are shown to be constructive, in the sense that these may be employed to generate convex yield functions (examples of which are also included).

Beyond the issue of convexity, the central purpose of this paper is the proposal of a yield criterion [see eqns. (6)-(9)]. This meets all of the above-listed requirements and can be viewed as a generalization of the following criteria: von Mises, Drucker-Prager, Tresca, modified Tresca, Coulomb-Mohr, modified Cam-clay, Deshpande and Fleck (2000), Rankine, and Ottosen (1977) (the last two for the deviatoric section). Obviously, the criterion may account for situations which cannot be described by the simple criteria to which it reduces in particular cases. Several examples of this may be found in the field of granular media, where several *ad hoc* yield conditions have been proposed, which may describe *one peculiar material, but cannot describe another*. In the present paper, it is shown with several examples that our yield criterion provides a unified description for a extremely broad class of quasi-brittle and frictional materials. Beyond the evident interest in generalization, there is a specific motivation for advocating the necessity of having a single criterion describing different materials. This lies in the fact that *during hardening, a yield surface may evolve from the shape typical of a certain material to that typical of another*. An evident example of this behaviour can be found in the field of granular materials, referring in particular to metal powders. These powders become cohesive during compaction, so that the material is initially a true granular material, but becomes finally a porous metal, whose porosity may be almost completely eliminated through sintering. The key to simulate this process is plasticity theory, so that a yield function must be employed evolving from the typical shape of a granular material ('triangular' deviatoric and 'drop-shaped' meridian sections), to that of a porous metal (circular deviatoric and elliptic meridian sections) and, in case of sintering, to that of a fully-dense metal (von Mises criterion). Another example of extreme shape variation of yield function during hardening is the process of decohesion of a rock-like material due to damage accumulation, a situation in a sense opposite to that described above. Evidently, a continuous distortion of the yield surface can be described employing the criterion proposed in this paper and simply making material parameters depend on hardening.

2 A premise on Haigh-Westergaard representation

The analysis will be restricted to isotropic behaviour, therefore the Haigh-Westergaard representation of the yield locus is employed (Hill, 1950). This is well-known, so that we limit the presentation here to a few remarks that may be useful in the following. First,

we recall that:

- $\mathcal{A}1$. a single point in the Haigh-Westergaard space is representative of the infinite (to the power three) stress tensors having the same principal values;
- $\mathcal{A}2$. due to the arbitrariness in the ordering of the eigenvalues of a tensor, six different points correspond in the Haigh-Westergaard representation to a given stress tensor. As a result, the yield surface results symmetric about the projections of the principal axes on the deviatoric plane (Fig. 1);
- $\mathcal{A}3$. the Haigh-Westergaard representation preserves the scalar product only between coaxial tensors;
- $\mathcal{A}4$. a convex yield surface —for a material with a fixed yield strength under triaxial compression— must be internal to the two limit situations shown in Fig. 1 (Haythornthwaite, 1985). Note that the inner bound will be referred as ‘the Rankine limit’.

Due to isotropy, the analysis of yielding can be pursued fixing once and for all a reference system and restricting to all stress tensors diagonal in this system. We will refer to this setting as to the Haigh-Westergaard representation. When tensors (for instance, the yield function gradient) coaxial to the reference system are represented, the scalar product is preserved, property $\mathcal{A}3$. In the Haigh-Westergaard representation, the hydrostatic and

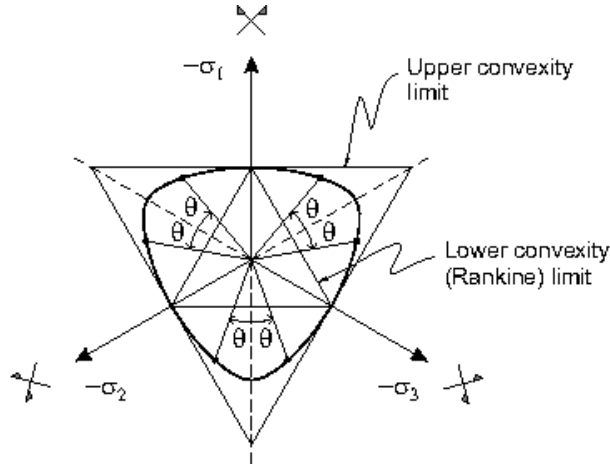


Figure 1: Deviatoric section: definition of angle θ , symmetries, lower and upper convexity bounds.

deviatoric stress components are defined by the invariants

$$p = -\frac{\text{tr } \boldsymbol{\sigma}}{3}, \quad q = \sqrt{3J_2}, \quad (1)$$

where

$$J_2 = \frac{1}{2} \mathbf{S} \cdot \mathbf{S}, \quad \mathbf{S} = \boldsymbol{\sigma} - \frac{\text{tr } \boldsymbol{\sigma}}{3} \mathbf{I}, \quad (2)$$

in which \mathbf{S} is the deviatoric stress, \mathbf{I} is the identity tensor, a dot denotes scalar product and tr denotes the trace operator, so that $\mathbf{A} \cdot \mathbf{B} = \text{tr } \mathbf{A} \mathbf{B}^T$, for every second-order tensors \mathbf{A} and \mathbf{B} . The position of the stress point in the deviatoric plane is singled out by the Lode (1926) angle θ defined as

$$\theta = \frac{1}{3} \cos^{-1} \left(\frac{3\sqrt{3}}{2} \frac{J_3}{J_2^{3/2}} \right), \quad J_3 = \frac{1}{3} \text{tr } \mathbf{S}^3, \quad (3)$$

so that $\theta \in [0, \pi/3]$. As a consequence of property (A2) of the Haigh-Westergaard representation, a single value of θ corresponds to six different points in the deviatoric plane (Fig. 1). The following gradients of the invariants, that will be useful later,

$$\begin{aligned} \frac{\partial p}{\partial \boldsymbol{\sigma}} &= -\frac{1}{3} \mathbf{I}, \quad \frac{\partial J_2}{\partial \boldsymbol{\sigma}} = \mathbf{S}, \quad \frac{\partial J_3}{\partial \boldsymbol{\sigma}} = \mathbf{S}^2 - \frac{\text{tr } \mathbf{S}^2}{3} \mathbf{I}, \\ \frac{\partial \theta}{\partial \boldsymbol{\sigma}} &= -\frac{9}{2q^3 \sin 3\theta} \left(\mathbf{S}^2 - \frac{\text{tr } \mathbf{S}^2}{3} \mathbf{I} - q \frac{\cos 3\theta}{3} \mathbf{S} \right), \end{aligned} \quad (4)$$

can be obtained from well-known formulae (e.g. Truesdell and Noll, 1965, Sect. 9) using the identity

$$\frac{\partial \mathbf{S}}{\partial \boldsymbol{\sigma}} = \mathbf{I} \underline{\otimes} \mathbf{I} - \frac{1}{3} \mathbf{I} \otimes \mathbf{I}, \quad (5)$$

where the symbol \otimes denotes the usual dyadic product and $\mathbf{I} \underline{\otimes} \mathbf{I}$ is the symmetrizing fourth-order tensor, defined for every tensor \mathbf{A} as $\mathbf{I} \underline{\otimes} \mathbf{I}[\mathbf{A}] = (\mathbf{A} + \mathbf{A}^T)/2$. Note that $\partial \theta / \partial \boldsymbol{\sigma}$ is orthogonal to \mathbf{I} and to the deviatoric stress \mathbf{S} .

3 A new yield function

We propose the seven-parameters yield function $F : \text{Sym} \rightarrow \mathbb{R} \cup \{+\infty\}$ defined as:

$$F(\boldsymbol{\sigma}) = f(p) + \frac{q}{g(\theta)}, \quad (6)$$

where the dependence on the stress $\boldsymbol{\sigma}$ is included in the invariants p , q and θ , eqns (1) and (3), through the ‘meridian’ function

$$f(p) = \begin{cases} -Mp_c \sqrt{(\Phi - \Phi^m) [2(1 - \alpha)\Phi + \alpha]} & \text{if } \Phi \in [0, 1], \\ +\infty & \text{if } \Phi \notin [0, 1], \end{cases} \quad (7)$$

where

$$\Phi = \frac{p + c}{p_c + c}, \quad (8)$$

describing the pressure-sensitivity³ and the ‘deviatoric’ function

$$g(\theta) = \frac{1}{\cos \left[\beta \frac{\pi}{6} - \frac{1}{3} \cos^{-1} (\gamma \cos 3\theta) \right]}, \quad (9)$$

describing the Lode-dependence of yielding. The seven, non-negative material parameters:

$$\underbrace{M > 0, p_c > 0, c \geq 0, 0 < \alpha < 2, m > 1}_{\text{defining } f(p)}, \quad \underbrace{0 \leq \beta \leq 2, 0 \leq \gamma < 1}_{\text{defining } g(\theta)}, \quad (10)$$

define the shape of the associated (single, smooth) yield surface. In particular, M controls the pressure-sensitivity, p_c and c are the yield strengths under isotropic compression and tension, respectively. Parameters α and m define the distortion of the meridian section, whereas β and γ model the shape of the deviatoric section. Note that the deviatoric function describes a piecewise linear deviatoric surface in the limit $\gamma \rightarrow 1$. Finally, it is important to remark that within the interval of $\beta \in [0, 2]$ the yield function is convex independently of the values assumed by parameter γ . Convexity requirements, that will be proved later, impose a broader variation of β than (10)₆, but the interval where β may range becomes a function of γ . In particular, the yield function is convex when

$$2 - \mathcal{B}(\gamma) \leq \beta \leq \mathcal{B}(\gamma), \quad (11)$$

where function $\mathcal{B}(\gamma)$ takes values within the interval $]2, 4]$, when γ ranges in $[0, 1[$ and is defined as

$$\mathcal{B}(\gamma) = 3 - \frac{6}{\pi} \tan^{-1} \frac{1 - 2 \cos z - 2 \cos^2 z}{2 \sin z (1 - \cos z)} \Big|_{z=2/3(\pi - \cos^{-1} \gamma)}. \quad (12)$$

The yield function (6) corresponds to the following yield surface:

$$q = -f(p)g(\theta), \quad p \in [-c, p_c], \quad \theta \in [0, \pi/3], \quad (13)$$

which makes explicit the fact that $f(p)$ and $g(\theta)$ define the shape of the meridian and deviatoric sections, respectively.

The yield surface (13) is sketched in Figs. 2-3 for different values of the seven above-defined material parameters (non-dimensionalization is introduced through division by p_c in Fig. 2). In particular, meridian sections are reported in Figs. 2 ($g(\theta) = 1$ has been taken), whereas Fig. 3 pertains to deviatoric sections.

³The meridian function can be written in an alternative form by using the Macauley bracket operator, defined for every scalar α as $\langle \alpha \rangle = \max\{0, \alpha\}$, and the indicator function $\chi_{[0,1]}(\Phi)$, which takes the

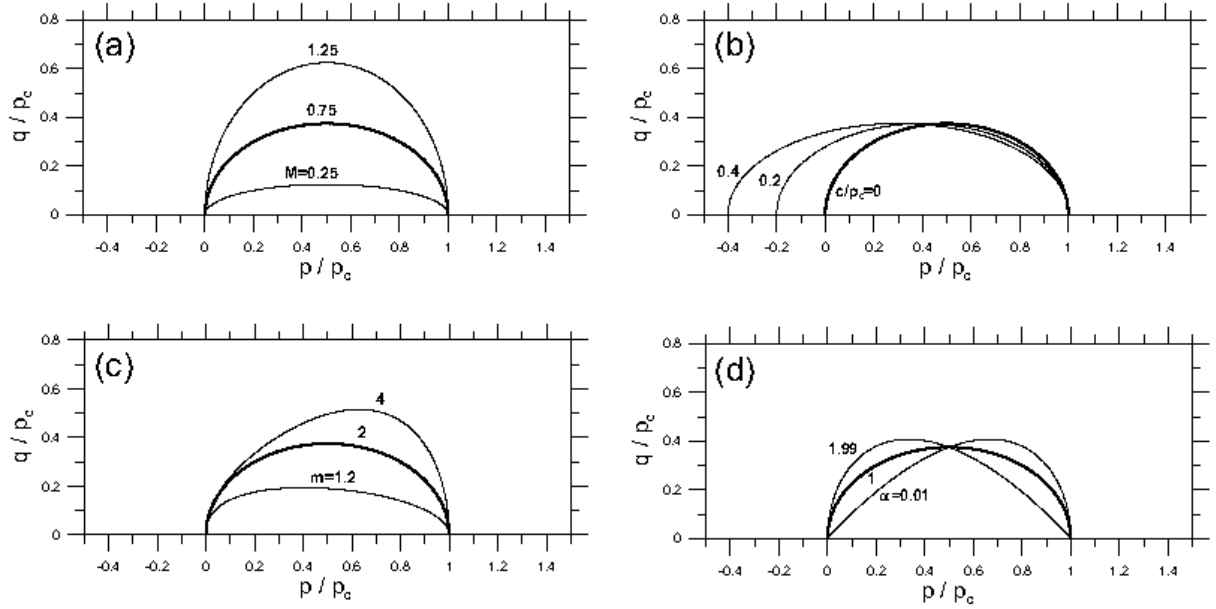


Figure 2: Meridian section: effects related to the variation of parameters M (a), c/p_c (b), m (c), and α (d).

As a reference, the case corresponding to the modified Cam-clay introduced by Roscoe and Burland (1968) and Schofield and Wroth (1968) and corresponding to $\beta = 1$, $\gamma = 0$, $\alpha = 1$, $m = 2$, and $c = 0$ is reported in Fig. 2 as a solid line, for $M = 0.75$. The distortion of meridian section reported in Fig. 2 (a) —where $M = 0.25, 0.75, 1.25$ — can also be obtained within the framework of the modified Cam-clay, whereas the effect of an increase in cohesion reported in Fig. 2 (b) —where $c/p_c = 0, 0.2, 0.4$ — may be employed to model the gain in cohesion consequent to plastic strain, during compaction of powders.

The shape distortion induced by the variation of parameters m and α , Fig. 2 (c) —where $m = 1.2, 2, 4$ — and (d) —where $\alpha = 0.01, 1.00, 1.99$ — is crucial to fit experimental results relative to frictional materials.

A unique feature of the proposed model is the possibility of extreme shape distortion of the deviatoric section, which may range between the upper and lower convexity limits, and approach Tresca, von Mises and Coulomb-Mohr. This is sketched in Fig. 3, where to simplify reading of the figure, function $g(\theta)$ has been normalized through division by $g(\pi/3)$, so that all deviatoric sections coincide at the point $\theta = \pi/3$. The use of

value 0 when $\Phi \in [0, 1]$ and is equal to $+\infty$ otherwise

$$f(p) = -Mp_c \sqrt{\left(\tilde{\Phi} - \tilde{\Phi}^m\right) \left[2(1 - \alpha)\tilde{\Phi} + \alpha\right] + \chi_{[0,1]}(\Phi)}, \quad \tilde{\Phi} = \langle \Phi \rangle - \langle \Phi - 1 \rangle.$$

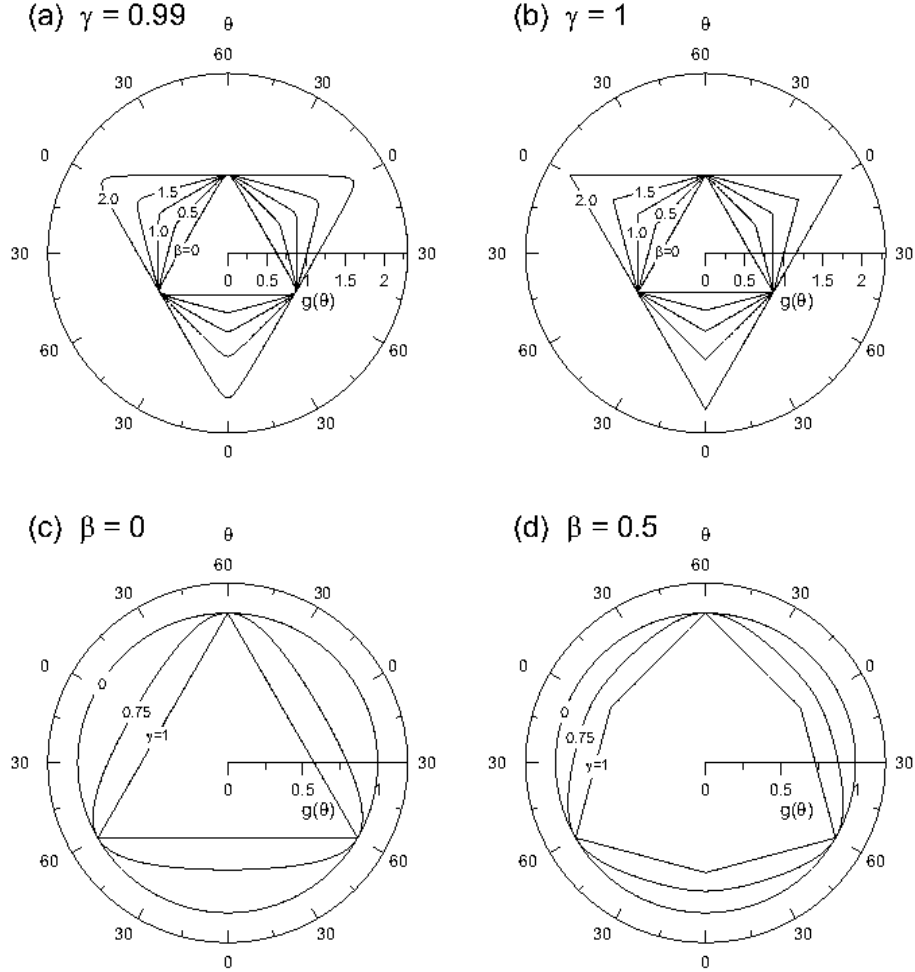


Figure 3: Deviatoric section: effects related to the variation of β and γ . Variation of $\beta = 0, 0.5, 1, 1.5, 2$ at fixed $\gamma = 0.99$ (a) and $\gamma = 1$ (b). Variation of $\gamma = 1, 0.75, 0$ at fixed $\beta = 0$ (c) and $\beta = 0.5$ (d).

our model may therefore allow one to simply obtain a convex, smooth approximation of several yielding criteria (Tresca and Coulomb-Mohr, for instance). If this may be not substantial from theoretical point of view, it clearly avoids the necessity of introducing independent yielding mechanisms.

Parameter γ is kept fixed in Figs. 3 (a) and (b) and equal to 0.99 and 1, respectively, whereas parameter β is fixed in Figs. 3 (c) and (d) and equal to 0 and 1/2. Therefore, figures (a) and (b) demonstrate the effect of the variation in β ($= 0, 0.5, 1, 1.5, 2$) which makes possible a distortion of the yield surface from the upper to lower convexity limits going through Tresca and Coulomb-Mohr shapes. The role played by γ ($= 1, 0.75, 0$) is investigated in figures (c) and (d), from which it becomes evident that γ has a smoothing effect on the corners, emerging in the limit $\gamma = 1$. The von Mises (circular) deviatoric

section emerges when $\gamma = 0$.

The yield surface in the biaxial plane σ_1 versus σ_2 , with $\sigma_3 = 0$ is sketched in Fig. 4, where axes are normalized through division by the uniaxial tensile strength f_t . In particular, the figure pertains to $M = 0.75$, $p_c = 50c$, $m = 2$, and $\alpha = 1$, whereas $\gamma = 0.99$ is fixed and β is equal to $\{0, 0.5, 1, 1.5, 2\}$ in Fig. 4 (a) and, vice-versa, $\beta = 0$ is fixed and γ is equal to $\{0, 0.75, 0.99\}$ in Fig. 4 (b).

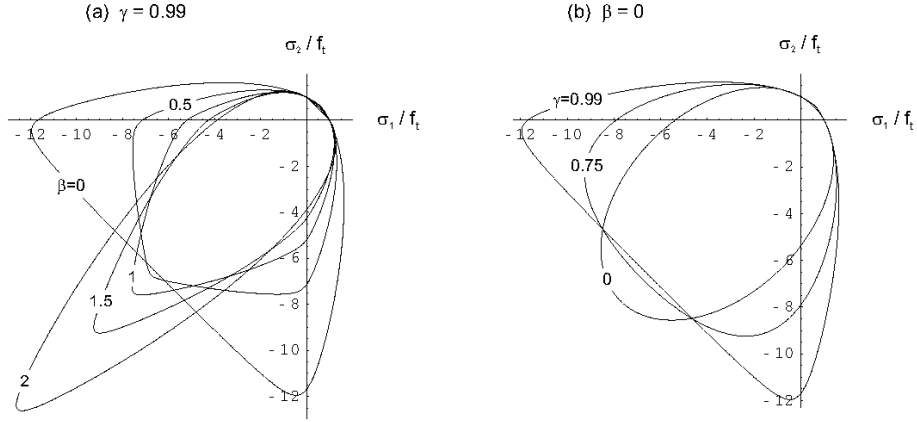


Figure 4: Yield surface in the biaxial plane σ_1/f_t vs. σ_2/f_t , with $\sigma_3 = 0$. Variation of $\beta = 0, 0.5, 1, 1.5, 2$ at fixed $\gamma = 0.99$ (a) and variation of $\gamma = 0, 0.75, 0.99$ at fixed $\beta = 0$ (b).

3.1 Smoothness of the yield surface

Smoothness of yield surface (13) within the interval of material parameters defined in (10)-(11) can be proved considering the yield function gradient. This can be obtained from (4) in the form

$$\frac{\partial F}{\partial \boldsymbol{\sigma}} = a(p) \mathbf{I} + b(\theta) \tilde{\mathbf{S}} + c(\theta) \tilde{\mathbf{S}}^\perp, \quad (14)$$

where

$$\tilde{\mathbf{S}} = \sqrt{\frac{3}{2}} \frac{\mathbf{S}}{q}, \quad \tilde{\mathbf{S}}^\perp = -\frac{\sqrt{2}}{\sqrt{3}q} \frac{\partial \theta}{\partial \boldsymbol{\sigma}} = \frac{1}{\sin 3\theta} \left[\sqrt{6} \left(\tilde{\mathbf{S}}^2 - \frac{1}{3} \mathbf{I} \right) - \cos 3\theta \tilde{\mathbf{S}} \right], \quad (15)$$

and

$$\begin{aligned} a(p) &= -\frac{1}{3} \frac{\partial f(p)}{\partial p} = \frac{Mp_c}{3(p_c + c)} \frac{(1 - m\Phi^{m-1}) [2(1 - \alpha)\Phi + \alpha] + 2(1 - \alpha)(\Phi - \Phi^m)}{2\sqrt{(\Phi - \Phi^m) [2(1 - \alpha)\Phi + \alpha]}}, \\ b(\theta) &= \sqrt{\frac{3}{2}} \frac{1}{g(\theta)}, \\ c(\theta) &= -\frac{\sqrt{3}\gamma \sin 3\theta}{\sqrt{2}\sqrt{1 - \gamma^2 \cos^2 3\theta}} \sin \left[\beta \frac{\pi}{6} - \frac{1}{3} \cos^{-1}(\gamma \cos 3\theta) \right]. \end{aligned} \quad (16)$$

It should be noted that $c(0) = c(\pi/3) = 0$ and that $\tilde{\mathbf{S}}$ and $\tilde{\mathbf{S}}^\perp$ are unit norm, coaxial and normal to each other tensors⁴. Coaxiality and orthogonality are immediate properties, whereas the proof that $|\tilde{\mathbf{S}}^\perp| = 1$ is facilitated when the following identities are kept into account

$$\tilde{\mathbf{S}}^3 - \frac{1}{2}\tilde{\mathbf{S}} - \frac{\cos 3\theta}{3\sqrt{6}}\mathbf{I} = \mathbf{0}, \quad \rightsquigarrow \quad \tilde{\mathbf{S}}^2 \cdot \tilde{\mathbf{S}}^2 = \frac{1}{2}, \quad (17)$$

the former of which is the Cayley-Hamilton theorem written for $\tilde{\mathbf{S}}$. Let us consider now from (14) the unit-norm yield function gradient

$$\mathbf{Q} = \frac{a}{\sqrt{3a^2 + b^2 + c^2}}\mathbf{I} + \frac{b}{\sqrt{3a^2 + b^2 + c^2}}\tilde{\mathbf{S}} + \frac{c}{\sqrt{3a^2 + b^2 + c^2}}\tilde{\mathbf{S}}^\perp, \quad (18)$$

defining, for stress states satisfying $F(\boldsymbol{\sigma}) = 0$, the unit normal to the yield surface. The following limits can be easily calculated

$$\lim_{\Phi \rightarrow 0^+} \mathbf{Q} = \frac{1}{\sqrt{3}}\mathbf{I}, \quad \lim_{\Phi \rightarrow 1^-} \mathbf{Q} = -\frac{1}{\sqrt{3}}\mathbf{I}, \quad (19)$$

so that the yield surface results to be smooth at the limit points where the hydrostatic axis is met. Moreover, smoothness of the deviatoric section of the yield surface is proved observing that

$$\lim_{\theta \rightarrow 0, \pi/3} \mathbf{Q} = \frac{a}{\sqrt{3a^2 + b^2}}\mathbf{I} + \frac{b}{\sqrt{3a^2 + b^2}}\tilde{\mathbf{S}}, \quad (20)$$

where $\tilde{\mathbf{S}}$ and b are evaluated at $\theta = 0$ and $\theta = \pi/3$, and noting that $\tilde{\mathbf{S}}$ and $\tilde{\mathbf{S}}^\perp$ are coaxial, deviatoric tensors so that they are represented by two orthogonal vectors in the deviatoric plane in the Haigh-Westergaard stress space. We observe, finally, that limits (19) do not hold true when α equals 0 and 2 and that limits (20) does not hold true when $\gamma = 1$. In particular, a corner appears at the intersection of the yield surface with the hydrostatic axis in the former case and the deviatoric section becomes piecewise linear in the latter.

3.2 Reduction of yield criterion to known cases

The yield function (6)-(9) reduces to almost all⁵ ‘classical’ criteria of yielding. These can be obtained as limit cases in the way illustrated in Tab. 1 where the modified Tresca criterion was introduced by Drucker (1953), whereas the Haigh-Westergaard representation of the Coulomb-Mohr criterion was proposed by Shield (1955). In Tab. 1 parameter

⁴ Note that $c\tilde{\mathbf{S}}^\perp = \mathbf{0}$ at $\theta = 0, \pi/3$. This can be deduced from the fact that $|\tilde{\mathbf{S}}^\perp| = 1$ and $c = 0$ for $\theta = 0, \pi/3$ or, alternatively, can be proved directly observing that for $\theta = 0, \pi/3$ the deviatoric stress can be generically written as $\{S_1, -S_1/2, -S_1/2\}$, unless all (uninfluential) permutations of components.

⁵A remarkable exception is the isotropic Hill (1950 b) criterion, corresponding to a Tresca criterion rotated of $\pi/6$ in the deviatoric plane.

r denotes the ratio between the uniaxial strengths in compression (taken positive) and tension, indicated by f_c and f_t , respectively. We note that for real materials $r \geq 1$ and that we did not explicitly consider the special cases of no-tension $f_t = 0$ or granular $f_t = f_c = 0$ materials [which anyway can be easily incorporated as limits of (6)-(9)].

We note that the expression of the Tresca criterion which follows from (6)-(9) in the limits specified in Tab. 1, was provided also by Bardet (1990) and answers—in a positive way—the question (raised by Salençon, 1974) if a proper⁶ form of the criterion in terms of stress invariants exist.

The Mohr-Coulomb limit merits a special mention. In fact, if the following values of the parameters are selected

$$\alpha = 0, \quad c = \frac{f_c [\cos(\beta \frac{\pi}{6} - \frac{\pi}{3}) + \cos \beta \frac{\pi}{6}]}{3r \cos(\beta \frac{\pi}{6} - \frac{\pi}{3}) - 3 \cos \beta \frac{\pi}{6}}, \quad M = \frac{3 [r \cos(\beta \frac{\pi}{6} - \frac{\pi}{3}) - \cos \beta \frac{\pi}{6}]}{\sqrt{2}(r + 1)}, \quad (21)$$

and then the limits

$$\gamma \longrightarrow 1, \quad p_c = f_c m \longrightarrow \infty, \quad (22)$$

are performed, a three-parameters generalization of Coulomb-Mohr criterion is obtained, which reduces to the latter criterion in the special case when β is selected in the form specified in Tab. 1 (yielding an expression noted also by Chen and Saleeb, 1982). The cases reported in Tab. 1 refer to situations in which the criterion (6)-(9) reduces to known yield criteria both in terms of function $f(p)$ and of function $g(\theta)$. It is however important to mention that the Lode's dependence function $g(\theta)$ reduces also to well-known cases, but in which the pressure-sensitivity cannot be described by the meridian function (7). These are reported in Tab. 2. It is important to mention that the form of our function $g(\theta)$, eqn. (9), was indeed constructed as a generalization of the deviatoric function introduced by Ottosen (1977).

3.3 A comparison with experiments

A brief comparison with experimental results referred to several materials is reported below. We limit the presentation to a few representative examples demonstrating the extreme flexibility of the proposed model to fit experimental results. In particular, we concentrate on the meridian section, whereas only few examples are provided for the deviatoric section, which has a shape so deformable and ranging between well-known

⁶The expression

$$f(\boldsymbol{\sigma}) = 4J_2^3 - 27J_3^2 - 36k^2J_2^2 + 96k^4J_2 - 64k^6,$$

where k is the yield stress under shear (i.e. $k = f_t/2$), reported in several textbooks on plasticity, is definitively wrong. This can be easily verified taking a stress state belonging to one of the planes defining the Tresca criterion, but outside the yield locus, for instance, the point $\{\sigma_1 = 0, \sigma_2 = -2k, \sigma_3 = 2k\}$, corresponding to $J_2 = 4k^2$ and $J_3 = 0$. Obviously, the point lies well outside the yield locus, but satisfies $f(\boldsymbol{\sigma}) = 0$, when the above, wrong, yield function is used.

Table 1: Yield criteria obtained as special cases of (6)-(9), $r = f_c/f_t$ and f_c and f_t are the uniaxial strengths in compression and tension, respectively.

Criterion	Meridian function $f(p)$	Deviatoric function $g(\theta)$
von Mises	$\alpha = 1, \quad m = 2,$ $M = \frac{2f_t}{p_c}, \quad c = p_c \longrightarrow \infty$	$\beta = 1, \gamma = 0$
Drucker-Prager	$\alpha = 0, \quad M = \frac{3(r-1)}{\sqrt{2}(r+1)},$ $c = \frac{2f_c}{3(r-1)}, \quad p_c = f_c m \longrightarrow \infty$	as for von Mises
Tresca	as for von Mises, except that $M = \frac{\sqrt{3}f_t}{p_c}$	$\beta = 1, \gamma \longrightarrow 1$
mod. Tresca	as for Drucker-Prager, except that $M = \frac{3\sqrt{3}(r-1)}{2\sqrt{2}(r+1)}$	as for Tresca
Coulomb-Mohr	as for Drucker-Prager, except that $M = \frac{3 \left[r \cos \left(\beta \frac{\pi}{6} - \frac{\pi}{3} \right) - \cos \beta \frac{\pi}{6} \right]}{\sqrt{2}(r+1)}$ $c = \frac{f_c \left[\cos \left(\beta \frac{\pi}{6} - \frac{\pi}{3} \right) + \cos \beta \frac{\pi}{6} \right]}{3r \cos \left(\beta \frac{\pi}{6} - \frac{\pi}{3} \right) - 3 \cos \beta \frac{\pi}{6}}$	$\beta = \frac{6}{\pi} \tan^{-1} \frac{\sqrt{3}}{2r+1},$ $\gamma \longrightarrow 1$
mod. Cam-clay	$m = 2, \alpha = 1, c = 0$	as for von Mises

Table 2: Deviatoric yield functions obtained as special cases of (9)

Criterion	Deviatoric function $g(\theta)$
Lower convexity (Rankine)	$\beta = 0, \gamma \rightarrow 1$
Upper convexity	$\beta = 2, \gamma \rightarrow 1$
Ottosen	$\beta = 0, 0 \leq \gamma < 1$

forms that fitting experiments is a-priori expected. Results on the biaxial plane $\sigma_1 - \sigma_2$ are also included. All values of material parameters defining the yield function (6)-(9) employed to fit experimental data may be useful as a reference and are reported in Appendix A.

Typical of soils are the experimental results reported in Fig. 5, on Aio dry sand and Weald clay, taken, respectively, from Yasufuku et al. (1991, their Fig. 10a) and Parry (reported by Wood, 1990, their Fig. 7.22, so that p_e is the equivalent consolidation pressure in Fig. 5(b)). Note that the upper plane of the graphs refers to triaxial compression ($\theta = \pi/3$), whereas triaxial extension is reported in the lower part of the graphs ($\theta = 0$). It may be concluded from the figure that experimental results can be easily fitted by our function $f(p)$, still maintaining a smooth intersection of the yield surface with p -axis.

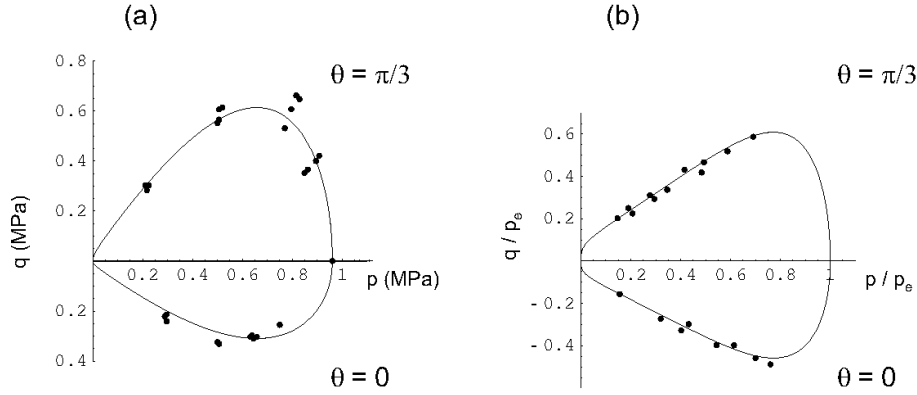


Figure 5: Comparison with experimental results relative to sand (Yasufuku et al. 1991) (a) and clay (Parry, reported by Wood, 1990) (b).

In addition to soils, the proposed function (6)-(9) can model yielding of porous ductile or cellular materials, metallic and composite powders, concrete and rocks. To further develop this point, a comparison with experimental results given by Sridhar and Fleck (2000) —their Figs. 5(b) and 9(c)— relative to ductile powders is reported in Fig. 6. In particular, Fig. 6 (a) is relative to an aluminum powder ($Al D_0=0.67, D=0.81$ in Sridhar and Fleck, their Fig. 5b), Fig. 6 (b) to an aluminum powder reinforced by 40 vol.%SiC

(Al-40%SiC $D_0=0.66$, $D=0.82$ in Sridhar and Fleck, their Fig. 5b), Fig. 6 (c) to a lead powder (0% steel in Sridhar and Fleck, their Fig. 9c), and Fig. 6 (d) to a lead shot-steel composite powder (20% steel in Sridhar and Fleck, their Fig. 9c). Beside the fairly good agreement between experiments and proposed yield function, we note that the aluminium powder has a behaviour —different from soils and lead-based powders— resulting in a meridian section of the yield surface similar to the early version of the Cam-clay model (Roscoe and Schofield, 1963).

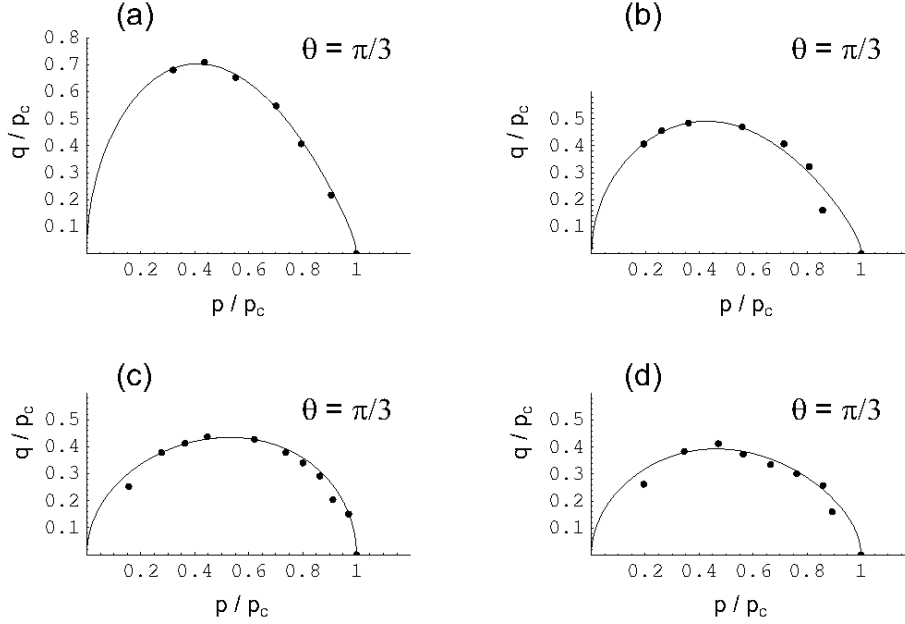


Figure 6: Comparison with experimental results relative to aluminium powder (a) aluminum composite powder (b), lead powder (c) and lead shot-steel composite powder(d), data taken from Sridhar and Fleck (2000).

Regarding concrete, among the many experimental results currently available, we have referred to Sfer et al. (2002, their Fig. 6) and to the Newman and Newman (1971) empirical relationship

$$\frac{\sigma_1}{f_c} = 1 + 3.7 \left(\frac{\sigma_3}{f_c} \right)^{0.86}, \quad (23)$$

where σ_1 and σ_3 are the maximum and minimum principal stresses at failure and f_c is the value of the ultimate uniaxial compressive strength. Small circles in Fig. 7 represents results obtained using relationship (23) in figure (a) and experimental results by Sfer et al. (2002) in figure (b); the approximation provided by the criterion (7)-(8) is also reported as a continuous line.

As far as rocks are concerned, we limit to a few examples. However, we believe that due to the fact that our criterion approaches Coulomb-Mohr, it should be particularly

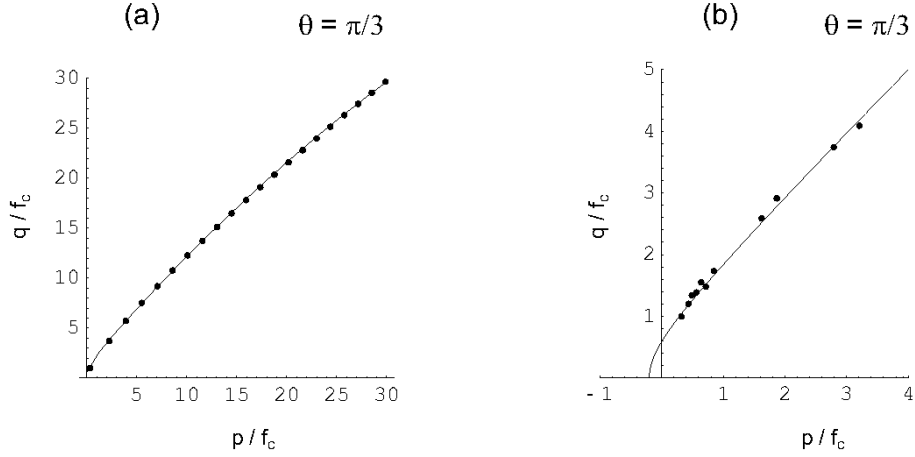


Figure 7: Comparison with the experimental relation (23) proposed by Newman and Newman (1971) (a) and with results by Sfer et al. (2002) (b).

suited for these materials. In particular, data taken from Hoek and Brown (1980, their pages. 143 and 144) are reported in Fig. 8 as small circles for two rocks, chert (Fig. 8 a) and dolomite (Fig. 8 b).

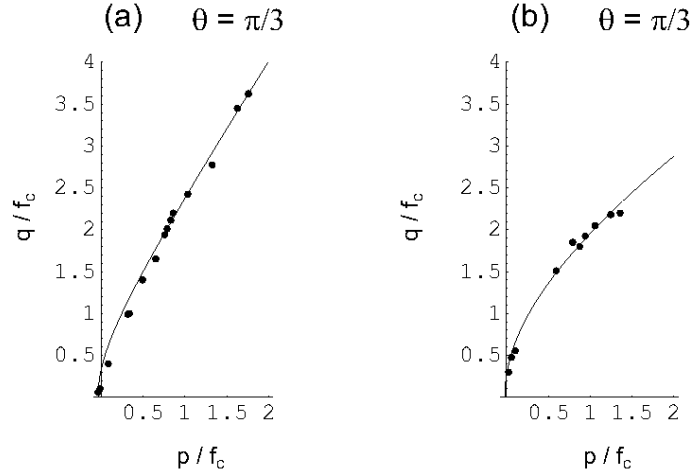


Figure 8: Comparison with experiments for rocks. Chert (a) and dolomite (b), data taken from Hoek and Brown (1980).

A few data on polymers are reported in Fig. 9—together with the fitting provided by our model—concerning polymethyl methacrylate (Fig. 9 a) and an epoxy binder (Fig. 9 b), taken from Ol'khovik (1983, their Fig. 5), see also Altenbach and Tushtev (2001, their Figs. 2 and 3).

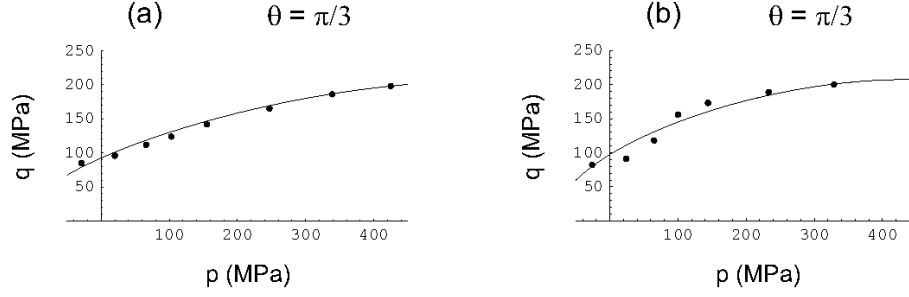


Figure 9: Comparison with experimental results for polymers. Methacrylate (a) and an epoxy binder (b), data taken from Ol'khovik (1983).

Finally, our model describes —with a different yield function— the same yield surface proposed by Deshpande and Fleck (2000) to describe the behaviour of metallic foams. In particular, the correspondence between parameters of our model (6)-(9) and of the yield surface proposed by Deshpande and Fleck [2000, their eqns. (2)-(3)] is obtained setting

$$\beta = 1, \quad \gamma = 0, \quad m = 2, \quad \alpha = 1,$$

and assuming the correlations given in Tab. 3.

Table 3: Correspondence between parameters of (6)-(9) and Deshpande and Fleck (2002) yield functions —the latter shortened as ‘DF model’— to describe the behaviour of metallic foams.

	Model (6)-(9)			DF model	
	M	c	p_c	Y	α
DF model Y, α	2α	$\frac{Y}{\alpha} \sqrt{1 + \left(\frac{\alpha}{3}\right)^2}$	$\frac{Y}{\alpha} \sqrt{1 + \left(\frac{\alpha}{3}\right)^2}$	—	—
Model (6)-(9) M, p_c, c	—	—	—	$\frac{cM}{2\sqrt{1 + \left(\frac{M}{6}\right)^2}}$	$\frac{M}{2}$

The proposed function (6)-(9) is also expected to model correctly yielding of porous ductile metals. As a demonstration of this, we present in Fig. 10 a comparison with the Gurson (1977) model. The Gurson yield function has a circular deviatoric section so that

$\beta = 1$ and $\gamma = 0$ in our model, in addition, we select

$$\alpha = 1, \quad m = 2, \quad p_c = c = \sigma_M \frac{2}{3q_2} \cosh^{-1} \frac{1 + q_3 f^2}{2f q_1}, \quad M = \sigma_M \frac{2}{p_c} \sqrt{1 + q_3 f^2 - 2f q_1}, \quad (24)$$

where f is the void volume fraction (taking the values $\{0.01, 0.1, 0.3, 0.6\}$ in Fig. 10), σ_M is the equivalent flow stress in the matrix material and $q_1 = 1.5$, $q_2 = 1$ and $q_3 = q_1^2$ are the parameters introduced by Tvergaard (1981, 1982). A good agreement between the two models can be appreciated from Fig. 10, increasing when the void volume fraction f increases.

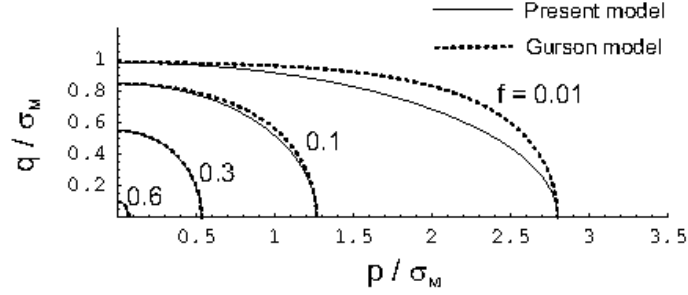


Figure 10: Comparison with the Gurson model at different values of void volume fraction f .

As far as the deviatoric section is regarded, we limit to two examples —reported in Fig. 11— concerning sandstone and dense sand, where the experimental data have been taken from Lade (1997, their Figs. 2 and 9a).

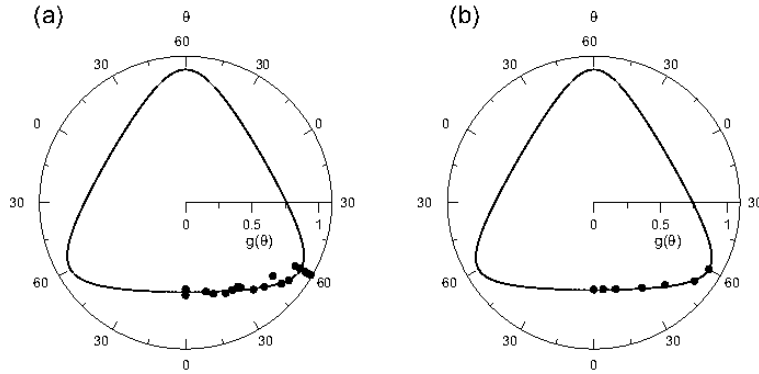


Figure 11: Comparison with experimental results relative to deviatoric section for sandstone (a) and dense sand (b) data taken from (Lade, 1997).

Experimental data referred to the biaxial plane $\sigma_3 = 0$ for grey cast iron and concrete (taken respectively from Coffin and Schenectady, 1950, their Fig. 5 and Tasuji et al. 1978, their Figs. 1 and 2) are reported in Fig. 12.

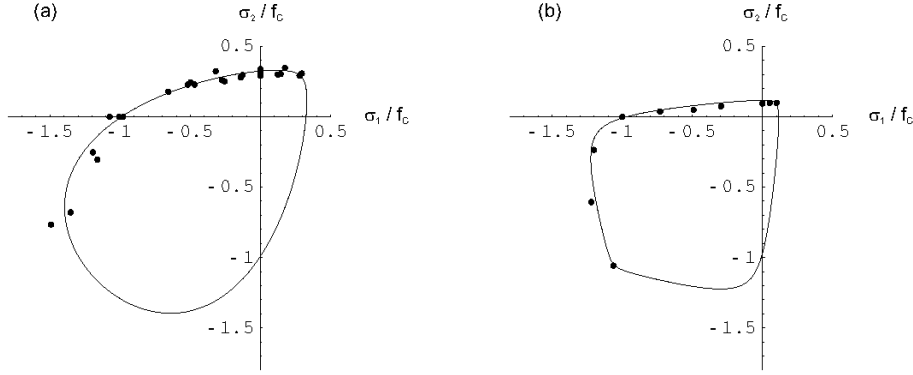


Figure 12: Comparison with experimental results on biaxial plane for cast iron (data taken from Coffin and Schenectady, 1950)(a) and concrete (data taken from Tasuji et al. 1978)(b).

4 On convexity of yield function and yield surface

Convexity of the yield function (6)-(9) within the range of parameters (10)-(11) was simply stated in the previous Section and still needs a proof. This will be given at the end of the present section as an application of a general proposition relating convexity of yield functions and surfaces that is given below.

We begin noting that while convexity of yield function implies convexity of the corresponding yield surface, the converse is usually false, namely, convexity of the level set of a function is unrelated to convexity of the function itself. As an example, let us consider the non-convex yield function

$$f(p, q) = \frac{p^4}{a^4} - \frac{p^2}{a^2} + \frac{q^2}{b^2}, \quad 0 \leq \frac{p}{a} \leq 1, \quad (25)$$

(where a and b are material parameters having the dimension of stress) which corresponds to a convex yield surface $f(p, q) = 0$, Fig. 13. After the pioneering work of de Finetti (1949), it became clear that convexity of *every* level set of a function represents its *quasi-convexity*, a property defining a class of functions much broader than the class of convex functions. In more detail, let us consider a function $f(\mathbf{x}) : U \rightarrow \mathbb{R}$, with U being a convex set, and its level sets

$$L_\alpha = \{\mathbf{x} \in U \mid f(\mathbf{x}) \leq \alpha\}, \quad (26)$$

so that:

f is quasi-convex if the level sets L_α are convex for every $\alpha \in \mathbb{R}$.

Now, the above definition of quasi-convexity is equivalent (Roberts and Varberg, 1973) to the definition

$$f[\lambda \mathbf{x} + (1 - \lambda) \mathbf{y}] \leq \max \{f(\mathbf{x}), f(\mathbf{y})\}, \quad \forall \mathbf{x}, \mathbf{y} \in U, \quad \forall \lambda \in [0, 1], \quad (27)$$

and, if f is continuous and differentiable, to

$$f(\mathbf{y}) \leq f(\mathbf{x}) \Rightarrow \nabla f(\mathbf{x}) \cdot (\mathbf{x} - \mathbf{y}) \geq 0, \quad \forall \mathbf{x}, \mathbf{y} \in U. \quad (28)$$

Convexity of the yield *surface* can be either accepted on the basis of experimental results, or on some engineering argumentation, such as for instance Drucker's postulate. Obviously, a convex yield locus can be expressed as a level set of a function, that generally may lack convexity and, even, quasi-convexity. For example, the level sets of function (25) are given in Fig. 13. It can be observed that while $f(p, q) = 0$ may perfectly serve

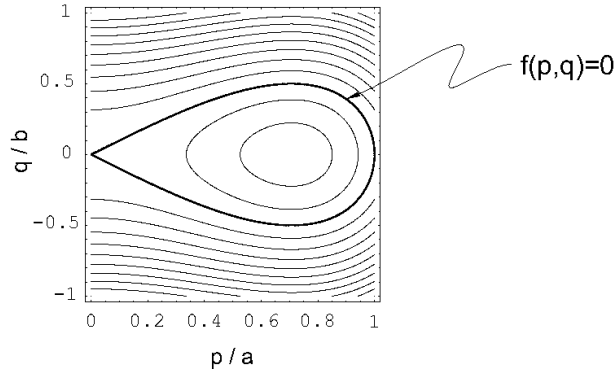


Figure 13: Level sets of function (25).

as a (convex) yield surface, the corresponding yield function even lacks quasi-convexity⁷. It is true that, in principle, a convex yield function can always be found to represent a convex yield surface, but to find this in a reasonably simple form may be an hard task. In other words, a number of yield functions that were formulated as an interpolation of experimental results still need a proof of convexity, even in cases where the corresponding yield locus is convex. The propositions that will be given below set some basis to provide these proofs.

4.1 A general result for a class of yield functions

The yield function (6)-(9) presented in the previous section may be viewed as an element of a family of models specified by the generic form (6). This family includes, among others, the models by Gudheus (1973), Argyris et al. (1974), Willam and Warnke (1975),

⁷As noted by Franchi et al. (1990), definition (28) is very similar to Drucker's postulate. However, Drucker's postulate merely prescribes the so-called normality rule of plastic flow and convexity of yield surface (Drucker, 1956, 1964). Quasi-convexity becomes a consequence of Drucker's postulate only in the special case —considered by Franchi et al. (1990)— in which convexity of yield surface implies convexity of all level sets of the corresponding function.

Eekelen (1980), Lin and Bazant (1986), Bardet (1990), Ehlers (1995), and Men  trety and Willam (1995) and Christensen (1997) and Christensen et al. (2002).

A general result is provided below showing that for the range of material parameters for which the Haigh-Westergaard representation of a yield surface (13) is convex, the function is also convex.

Proposition 1: Convexity of the yield *function* (6) is equivalent to convexity of the meridian and deviatoric sections of the corresponding yield *surface* (13) in the Haigh-Westergaard representation. In symbols:

$$\text{convexity of } F(\boldsymbol{\sigma}) = f(p) + \frac{q}{g(\theta)} \iff f'' \geq 0, \quad \& \quad g^2 + 2g'^2 - gg'' \geq 0, \quad (29)$$

where $g(\theta)$ is a positive function.

Proof. It is a well-known theorem of convex analysis (Ekeland and Temam, 1976) that the sum of two convex functions is also a convex function. Since q , p and θ are independent parameters, failure of convexity of $f(p)$ or $q/g(\theta)$ implies failure of convexity of $F(\boldsymbol{\sigma})$ and therefore convexity of both $f(p)$ and $q/g(\theta)$ are necessary and sufficient conditions for convexity of $F(\boldsymbol{\sigma})$.

Now, let us first analyze $f(p)$. The fact that convexity of $f(p)$ as a function of $\boldsymbol{\sigma}$ is equivalent to convexity of the meridian section follows from linearity of the trace operator, in view of the fact that $p = -\text{tr } \boldsymbol{\sigma}/3$.

Second, the fact that convexity of $q/g(\theta)$ as function of $\boldsymbol{\sigma}$ is equivalent to the convexity of the deviatoric section follows from the 3 lemmas listed below.

□

Lemma 1 (Hill, 1968): Convexity of an isotropic function of a symmetric (stress) tensor $\boldsymbol{\sigma}$ is equivalent to convexity of the corresponding function of the principal (stress) values σ_i ($i = 1, 2, 3$). In symbols, given:

$$\phi(\boldsymbol{\sigma}) = \tilde{\phi}(\sigma_1, \sigma_2, \sigma_3), \quad (30)$$

then:

$$\Delta \frac{\partial \phi}{\partial \boldsymbol{\sigma}} \cdot \Delta \boldsymbol{\sigma} \geq 0 \iff \sum_{i=1}^3 \Delta \frac{\partial \tilde{\phi}}{\partial \sigma_i} \Delta \sigma_i \geq 0, \quad (31)$$

where Δ denotes an ordered difference in the variables, so that, denoting with A and B two points in the tensor space

$$\Delta \frac{\partial \phi}{\partial \boldsymbol{\sigma}} \cdot \Delta \boldsymbol{\sigma} = \left(\frac{\partial \phi}{\partial \boldsymbol{\sigma}} \Big|_{\boldsymbol{\sigma}^A} - \frac{\partial \phi}{\partial \boldsymbol{\sigma}} \Big|_{\boldsymbol{\sigma}^B} \right) \cdot (\boldsymbol{\sigma}^A - \boldsymbol{\sigma}^B), \quad (32)$$

$$\Delta \frac{\partial \tilde{\phi}}{\partial \sigma_i} \Delta \sigma_i = \left(\frac{\partial \tilde{\phi}}{\partial \sigma_i} \Big|_{\{\sigma_1^A, \sigma_2^A, \sigma_3^A\}} - \frac{\partial \tilde{\phi}}{\partial \sigma_i} \Big|_{\{\sigma_1^B, \sigma_2^B, \sigma_3^B\}} \right) (\sigma_i^A - \sigma_i^B), \quad i = 1, 2, 3. \quad (33)$$

Proof. That convexity of ϕ implies convexity of $\tilde{\phi}$ is self-evident. The converse is not trivial and a proof was given by Hill (1968) with reference to an elastic strain energy function. The proof, omitted here for brevity, was later obtained also by Yang (1980) with explicit reference to a yield function. \square

Lemma 2: Given a generic isotropic function ϕ of the stress that can be expressed as

$$\phi(\sigma_1, \sigma_2, \sigma_3) = \tilde{\phi}(S_1, S_2), \quad (34)$$

where S_1 and S_2 are two of the principal components of deviatoric stress, i.e.

$$S_1 = \frac{1}{3}(2\sigma_1 - \sigma_2 - \sigma_3), \quad S_2 = \frac{1}{3}(-\sigma_1 + 2\sigma_2 - \sigma_3), \quad (35)$$

convexity of $\phi(\sigma_1, \sigma_2, \sigma_3)$ is equivalent to convexity of $\tilde{\phi}(S_1, S_2)$.

Proof. The proof follows immediately from the observation that the relation (35) between $\{S_1, S_2\}$ and $\{\sigma_1, \sigma_2, \sigma_3\}$ is linear. \square

Lemma 3: Convexity of

$$\frac{q}{g(\theta)} \quad (36)$$

as a function of S_1, S_2 is equivalent to the convexity of the deviatoric section in the Haigh-Westergaard space:

$$g^2 + 2g'^2 - gg'' \geq 0. \quad (37)$$

Proof. The Hessian of (36) is

$$\begin{aligned} \frac{\partial^2 q/g(\theta)}{\partial S_i \partial S_j} &= \frac{1}{g^3} \left[g^2 \frac{\partial^2 q}{\partial S_i \partial S_j} + q(2g'^2 - gg'') \frac{\partial \theta}{\partial S_i} \frac{\partial \theta}{\partial S_j} \right. \\ &\quad \left. - g g' \left(\frac{\partial q}{\partial S_i} \frac{\partial \theta}{\partial S_j} + \frac{\partial q}{\partial S_j} \frac{\partial \theta}{\partial S_i} + q \frac{\partial^2 \theta}{\partial S_i \partial S_j} \right) \right], \end{aligned} \quad (38)$$

where i and j range between 1 and 2 and all functions q and θ are to be understood as functions of S_1 and S_2 only. Derivatives of q may be easily calculated to be

$$\frac{\partial q}{\partial S_i} = 2S_i - (-1)^i m_i, \quad \frac{\partial^2 q}{\partial S_i \partial S_j} = \frac{27}{4q^3} m_i m_j, \quad (39)$$

where indices are not summed and vector \mathbf{m} has the components

$$\{\mathbf{m}\} = \{S_2, -S_1\}. \quad (40)$$

The derivatives of θ can be performed through $\cos 3\theta$, eqn. (3)₁, noting that

$$\begin{aligned} \frac{\partial \theta}{\partial S_i} &= \frac{-1}{3 \sin 3\theta} \frac{\partial \cos 3\theta}{\partial S_i}, \\ \frac{\partial^2 \theta}{\partial S_i \partial S_j} &= \frac{-1}{3 \sin 3\theta} \left(\frac{\cos 3\theta}{\sin^2 3\theta} \frac{\partial \cos 3\theta}{\partial S_i} \frac{\partial \cos 3\theta}{\partial S_j} + \frac{\partial^2 \cos 3\theta}{\partial S_i \partial S_j} \right), \end{aligned} \quad (41)$$

so that

$$\begin{aligned} &\frac{\partial q}{\partial S_i} \frac{\partial \theta}{\partial S_j} + \frac{\partial q}{\partial S_j} \frac{\partial \theta}{\partial S_i} + q \frac{\partial^2 \theta}{\partial S_i \partial S_j} \\ &= \frac{-1}{\sin 3\theta} \left[\frac{\partial^2 q \cos 3\theta}{\partial S_i \partial S_j} - \cos 3\theta \frac{\partial^2 q}{\partial S_i \partial S_j} + q \frac{\cos 3\theta}{\sin^2 3\theta} \frac{\partial \cos 3\theta}{\partial S_i} \frac{\partial \cos 3\theta}{\partial S_j} \right], \end{aligned} \quad (42)$$

where

$$\frac{\partial \cos 3\theta}{\partial S_i} = \frac{9\sqrt{3} \sin 3\theta}{2q^2} m_i, \quad \frac{\partial^2 q \cos 3\theta}{\partial S_i \partial S_j} = -27^2 \frac{J_3}{q^6} m_i m_j. \quad (43)$$

A substitution of (43) into (42) yields

$$\frac{\partial q}{\partial S_i} \frac{\partial \theta}{\partial S_j} + \frac{\partial q}{\partial S_j} \frac{\partial \theta}{\partial S_i} + q \frac{\partial^2 \theta}{\partial S_i \partial S_j} = 0, \quad (44)$$

so that we may conclude that the Hessian (38) can be written as

$$\frac{\partial^2 q/g(\theta)}{\partial S_i \partial S_j} = \frac{27}{4} \frac{(g^2 + 2g'^2 - gg'')}{q^3 g^3} m_i m_j. \quad (45)$$

Positive semi-definiteness of the Hessian (45) is condition (37), which, in turn, represents non-negativeness of the curvature (and thus convexity) of deviatoric section. \square

4.2 Applications of Proposition 1

The scope of this section is on one hand to prove the convexity of function (6)-(9) within the range (10)-(11) of material parameters, on the other hand to show that Proposition 1 is constructive, in the sense that can be used to invent convex yield functions. Let us begin with the first issue.

4.2.1 The proposed yield function (6)-(9)

First, we show that $f(p)$, eqn (6), is a convex function of p (so that the meridian section is convex) and, second, that the deviatoric section described by $g(\theta)$, eqn (9), is convex for the range of material parameters listed in (10)-(11). Therefore, as a conclusion from Proposition 1, function $F(\boldsymbol{\sigma})$ results to be convex.

A well-known result of convex analysis (Ekelan and Temam, 1976) states that function $f(p)$ is convex if and only if the restriction to its effective domain (i.e. $\Phi \in [0, 1]$) is convex. Moreover, the function Φ appearing in (8)₁ is a linear function of p so that convexity of $f(p)$ can be inferred from convexity of the corresponding function, say \tilde{f} , of Φ . Introducing for simplicity the function

$$h(\Phi) = (\Phi - \Phi^m) [2(1 - \alpha)\Phi + \alpha], \quad (46)$$

the convexity of function $\tilde{f}(\Phi)$ reduces to the condition

$$[h'(\Phi)]^2 - 2h''(\Phi)h(\Phi) \geq 0, \quad (47)$$

where

$$\begin{aligned} h'(\Phi) &= (1 - m\Phi^{m-1}) [2(1 - \alpha)\Phi + \alpha] + 2(1 - \alpha)(\Phi - \Phi^m), \\ h''(\Phi) &= -m(m - 1)\Phi^{m-2} [2(1 - \alpha)\Phi + \alpha] + 4(1 - \alpha)(1 - m\Phi^{m-1}). \end{aligned} \quad (48)$$

Fulfillment of eqn (47) can be now easily proven considering the inequality

$$h''(\Phi) \leq 4(1 - \alpha)(1 - m\Phi^{m-1}), \quad \forall \Phi \in [0, 1]. \quad (49)$$

It remains now to show convexity of $q/g(\theta)$. To this purpose, Proposition 1 can be employed, through substitution of (9) into the convexity condition eqn (37), thus yielding

$$\frac{1}{g(\theta)} + \frac{3\gamma \cos 3\theta}{\sqrt{1 - \gamma^2 \cos^2 3\theta}} \sin \left[\beta \frac{\pi}{6} - \frac{1}{3} \cos^{-1}(\gamma \cos 3\theta) \right] \geq 0, \quad (50)$$

where $\theta \in [0, \pi/3]$ and $g(\theta)$ is given by eqn (9). For values of γ belonging to the interval specified in (10)₇, condition (50) can be transformed into

$$\sin \left(\frac{\beta\pi}{6} - \frac{4}{3}x \right) + 2 \sin \left(\frac{\beta\pi}{6} + \frac{2}{3}x \right) \geq 0, \quad (51)$$

with $x \in [\cos^{-1} \gamma, \pi - \cos^{-1} \gamma]$ and then into

$$\frac{-1 + 2 \cos z + 2 \cos^2 z}{2 \sin z(1 - \cos z)} \sin \beta \frac{\pi}{6} + \cos \beta \frac{\pi}{6} \geq 0, \quad (52)$$

with $z \in [2/3 \cos^{-1} \gamma, 2/3(\pi - \cos^{-1} \gamma)]$, an inequality that can be shown to be verified within the interval of β specified in (11) and thus also within its subinterval (10)₆.

4.2.2 Generating convex yield functions

Proposition 1 can be easily employed to build convex yield functions within the class described by eqn (6). The simplest possibility is to maintain $f(p)$ in the form (7) and change the deviatoric function eqn (9). As a first proposal, we can introduce the following function

$$g(\theta) = [1 + \beta (1 + \cos 3\theta)]^{-1/n}, \quad (53)$$

instead of (9). This describes a smooth deviatoric section approaching (without reaching) the triangular (Rankine) shape when parameters $n > 0$ and $\beta \geq 0$ are varied. The yield function is convex within the range of parameters reported in Tab. 4 (see Appendix B for a proof). The yield function defined by eqns (7) and (53) does not possess the extreme

Table 4: Conditions for the convexity of deviatoric yield function (53).

$0 < n \leq 11/3$	$n \geq 11/3$
$\beta \leq \frac{n}{9-2n}$	$\beta \leq \left(-1 + \sqrt{1 + \frac{9(n-2)^2}{n^2(4n-13)}} \right)^{-1}$

deformability of (7) and (9) and does not admit Mohr-Coulomb and Tresca as limits, but results in a simple expression. The performance of the deviatoric shape of the yield

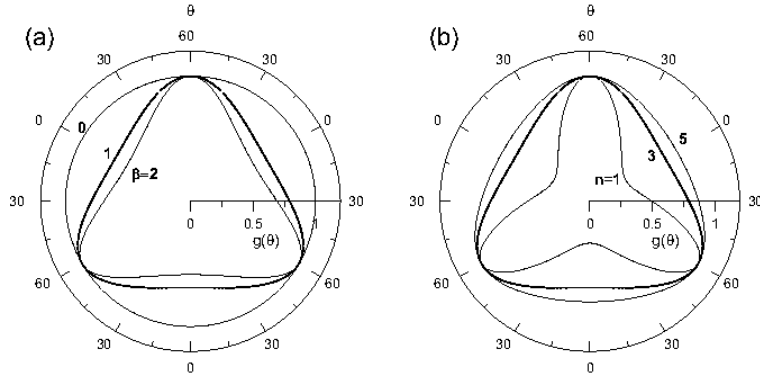


Figure 14: Deviatoric section (53): effects related to the variation of β (a) and n (b).

surface is analyzed in Fig. 14, where the solid lines correspond to the limit of convexity,

$\beta = 1$ and $n = 3$. The curves reported in Fig. 3 (a) are relative to the values of $\beta = 0, 1, 2$, whereas for Fig. 3 (b) n takes the values $\{1, 3, 5\}$.

A limitation of the yield surface described by eqns (7) and (53) is that the deviatoric section cannot be stretched until the Rankine limit. This can be easily emended assuming for $g(\theta)$ our expression (9) or that proposed by Willam and Warnke (1975) (see also Menétrey and Willam, 1995)

$$g(\theta) = \frac{2(1 - e^2) \cos \theta + (2e - 1) [4(1 - e^2) \cos^2 \theta + 5e^2 - 4e]^{0.5}}{4(1 - e^2) \cos^2 \theta + (2e - 1)^2}, \quad (54)$$

where $e \in]0.5, 1]$ is a material parameter, yielding in the limit $e \rightarrow 0.5$ the Rankine criterion and the von Mises criterion when $e = 1$.

It is already known that the deviatoric section of the yield surface corresponding to eqn (54) remains convex for any value of the parameter e ranging within the interval $]0.5, 1]$, so that —from Proposition 1— the function (6) equipped with the definition (54) of the function $g(\theta)$ is also convex.

As a final example, we can employ function $g(\theta)$ defined by the expression proposed by Gudheus (1973) and Argyris et al. (1974)

$$g(\theta) = \frac{2k}{1 + k + (1 - k) \cos 3\theta}, \quad (55)$$

where $k \in]0.777, 1]$ is a material parameter.

Otherwise, we can act on the meridian function. For instance, we can modify a Drucker-Prager criterion —which again fits in the framework described by eqn (6)— obtaining a non-circular deviatoric section described by eqn (9)

$$F(\boldsymbol{\sigma}) = -\Gamma(p + c) + q \cos \left[\beta \frac{\pi}{6} - \frac{1}{3} \cos^{-1}(\gamma \cos 3\theta) \right], \quad (56)$$

where c is the yield strength under isotropic tension and Γ is a material parameter, or by eqn (53)

$$F(\boldsymbol{\sigma}) = -\Gamma(p + c) + q[1 + \beta(1 + \cos 3\theta)]^{1/n}, \quad (57)$$

or by the Gudheus/Argyris condition (55)

$$F(\boldsymbol{\sigma}) = -\Gamma(p + c) + \frac{q}{2k} (1 + k + (1 - k) \cos 3\theta). \quad (58)$$

It may be noted that the yield criterion (58) has been employed by Laroussi et al. (2002) to describe the behaviour of foams. In all the above cases, Proposition 1 ensures that for the range of parameters in which the Haigh-Westergaard representation of the yield surface is convex, the yield function is also convex.

4.3 A note on the behaviour of concrete and a generalization of Proposition 1

In the modelling of concrete there is some experimental evidence that the deviatoric section starts close to the Rankine limit for low hydrostatic stress component and tends to approach a circle, when confinement increases. This effect has been described by Ottosen (1977) through a model which does not fit the general framework specified by eqn (6) and can be written in our notation in the form

$$F(\boldsymbol{\sigma}) = Aq^2 + B\frac{q}{g(\theta)} + C - p, \quad (59)$$

where $A > 0$, $B \geq 0$ and $C \leq 0$ are constants and $g(\theta)$ is in the form (9) with $\beta = 0$. The criterion is therefore defined by four parameters.

The above-expression (59) of the yield function suggests the following generalization of Proposition 1:

Proposition 2: Convexity of the yield function

$$F(\boldsymbol{\sigma}) = Aq^2 + B\frac{q}{g(\theta)} + f(p), \quad (60)$$

where A and B are positive constants, is equivalent to

$$f'' \geq 0, \quad \& \quad g^2 + 2g'^2 - gg'' \geq 0, \quad (61)$$

which in turn is equivalent to the convexity of the surface

$$B\frac{q}{g(\theta)} + f(p) = 0, \quad (62)$$

in the Haigh-Westergaard stress space.

Proof. Let us begin assuming that (61) holds true. In this condition Proposition 1 ensures that $f(p)$ and $q/g(\theta)$ are convex functions of $\boldsymbol{\sigma}$, so that (60) results the sum of three convex functions and its convexity follows. Vice-versa, failure of convexity of $f(p)$ immediately implies failure of convexity of (60) since p is independent of θ and q . Finally, let us assume that condition (61)₂ is violated, for a certain value, say $\tilde{\theta}$, of θ . The Hessian of

$$Aq^2 + Bq/g(\theta), \quad (63)$$

as a function of two components of deviatoric stress S_1 and S_2 , is given by eqn. (45) summed to a constant and positive definite matrix

$$3A \begin{bmatrix} 2 & 1 \\ 1 & 2 \end{bmatrix} + B \frac{27}{4} \frac{(g^2 + 2g'^2 - gg'')}{q^3 g^3} \begin{bmatrix} S_2^2 & -S_1 S_2 \\ -S_1 S_2 & S_1^2 \end{bmatrix}. \quad (64)$$

Considering now the Haigh-Westergaard representation, it is easy to understand that we can keep $\theta = \tilde{\theta}$ fixed and change S_1 and consequently S_2 so that S_1/S_2 remains constant. In this situation, while g and its derivatives remain fixed, the quantity

$$\frac{S_1^2}{q^3}, \quad (65)$$

in matrix (64) tends to $+\infty$ when S_1 tends to zero. Therefore, violation of $(61)_2$ cannot be compensated by a constant term and function (60) is not convex. \square

Proposition 2 provides the conditions for convexity of the Ottosen criterion. Moreover, the same proposition allows us to generalize our yield function (6)-(9) adding a q^2 term as in the Ottosen criterion. This leads immediately to

$$F(\boldsymbol{\sigma}) = A q^2 + B q \cos \left[\beta \frac{\pi}{6} - \frac{1}{3} \cos^{-1} (\gamma \cos 3\theta) \right] + f(p), \quad (66)$$

where $f(p)$ is given by eqn (7).

5 Conclusions

In the modelling of the inelastic behaviour of several materials, the knowledge of a smooth, convex yield surface approaching known-criteria and possessing an extreme shape variation to fit experimental results may be of undoubted utility. In particular, the fact that a yield function can continuously describe a transition between yield surfaces typical of different materials is of fundamental importance in modelling the de-cohesion due to damage of rock-like materials and the increase in cohesion during forming of powders. In the present paper, such a yield function has been proposed, which is shown to be capable of an accurate description of the behaviour of a broad class of materials including soils, concrete, rocks, powders, metallic foams, porous materials, and polymers. Moreover, in order to analyze convexity of our function, we have provided certain general results, holding for a broad class of yield conditions, which permit to infer convexity of the yield function from convexity of the yield surface.

Acknowledgments

The authors are grateful to Dr. Alessandro Gajo (University of Trento) for many useful discussions and suggestions. Financial support from University of Trento, Trento, Italy is gratefully acknowledged.

References

- [1] Altenbach, H., Tushtev, K., 2001. A new static failure criterion for isotropic polymers. *Mech. Compos. Mater.* 37, 475-482.
- [2] Argyris, J.H., Faust, G., Szimmat, J., Warnke, P., Willam, K., 1974. Recent developments in the finite element analysis of prestressed concrete reactor vessels. *Nucl. Eng. Des.* 28, 42-75.
- [3] Bardet, J.P. 1990. Lode dependences for isotropic pressure-sensitive elastoplastic materials. *J. Appl. Mech.* 57, 498-506.
- [4] Bishop, J.F.W. and Hill, R. 1951. A theory of the plastic distortion of a polycrystalline aggregate under combined stresses, *Phil. Mag.* 42, 414-427.
- [5] Chen, W.F., Saleeb, A.F. 1982. *Constitutive equations for engineering materials: elasticity and modelling.* Wiley & Sons, New York.
- [6] Christensen, R.M. 1997. Yield functions/failure criteria for isotropic materials. *Proc. R. Soc. Lond.* 453, 1473-1491.
- [7] Christensen, R.M., Freeman, D.c., DeTeresa, S.J. 2002. Failure criteria for isotropic materials, applications to low-density types. *Int. J. Solids Structures* 39, 973-982.
- [8] Coffin, L.F., Schenectady, N.Y., 1950. The flow and fracture of a brittle material. *J. Appl. Mech.* 17, 233-248.
- [9] De Finetti, B., 1949. Sulle stratificazioni convesse. *Ann. Mat. Pura Appl.* 30, 173-183.
- [10] Deshpande, V.S., Fleck, N.A., 2000. Isotropic constitutive models for metallic foams. *J. Mech. Phys. Solids* 48, 1253-1283.
- [11] Drucker, D.C., 1953. Limit analysis of two and three dimensional soil mechanics problems. *J. Mech. Phys. Solids* 1, 217-226.
- [12] Drucker, D.C., 1956. On uniqueness in the theory of plasticity. *Quart. Appl. Math.* XIV, 35-42.
- [13] Drucker, D.C., 1964. On the postulate of stability of material in the mechanics of continua. *J. de Mécanique* 3, 235-249.
- [14] Duvaut, G., Lions, J.L., 1976. *Inequalities in mechanics and physics.* Springer-Verlag, Berlin.
- [15] Eekelen, H.A.M., 1980. Isotropic yield surface in three dimensions for use in soil mechanics. *Int. J. Numer. Anal. Meth. Geomech.* 4, 89-101.
- [16] Ehelers, W., 1995. A single-surface yield function for geomaterials. *Arch. Appl. Mech.* 65, 246-259.
- [17] Ekeland, I., Temam, R., 1976. *Convex analysis and variational problems.* North-Holland, Amsterdam.

- [18] Franchi, A., Genna, F., Paterlini, F., 1990. Research note on quasi-convexity of the yield function and its relation to Drucker postulate. *Int. J. Plasticity* 6, 369-375.
- [19] Gudehus, G., 1973. Elastoplastische Stoffgleichungen für trockenen Sand. *Ingenieur-Archiv*. 42, 151-169.
- [20] Gurson, A.L., 1977. Continuum theory of ductile rupture by void nucleation and growth: part I, yield criteria and flow rules for porous ductile media. *Int. J. Engng. Mat. Tech.* 99, 2-15.
- [21] Haythornthwaite, R.M., 1985. A family of smooth yield surfaces. *Mechanics Research Communications* 12, 87-91.
- [22] Hill, R., 1950 a. The mathematical theory of plasticity. Clarendon Press, Oxford.
- [23] Hill, R., 1950 b. Inhomogeneous deformation of a plastic lamina in a compression test. *Phil. Mag.* 41, 733-744.
- [24] Hill, R., 1967. The essential structure of constitutive laws for metal composites and polycrystals. *J. Mech. Phys. Solids* 15, 79-95
- [25] Hill, R., 1968. On constitutive inequalities for simple materials-I. *J. Mech. Phys. Solids* 16, 229-242.
- [26] Hisieh, S.S., Ting, E.C., Chen, W.F., 1982. A plasticity-fracture model for concrete. *Int. J. Solids Structures* 18, 181-197.
- [27] Hoek, E., Brown, E.T., 1980. Underground excavations in rock. The Institution of Mining and Metallurgy, London.
- [28] Lade P.V., 1997. Modelling the strengths of engineering materials in three dimensions *Mech. Cohes. Frict. Mat.* 2, 339-356.
- [29] Lade, P.V., Kim, M.K., 1995. Single hardening constitutive model for soil, rock and concrete. *Int. J. Solids Structures* 32, 1963-1978.
- [30] Laroussi, M., Sab, K., Alaoui, A., 2002. Foam mechanics: nonlinear response of an elastic 3D-periodic microstructure. *Int. J. Solids Structures* 39, 3599-3623.
- [31] Lin, F-B., Bazant, Z., 1986. Convexity of smooth yield surface of frictional material. *ASCE J. Engng. Mech.* 112, 1259-1262.
- [32] Lode, W., 1926. Versuche über den Einfluß der mittleren Hauptspannung auf das Fließen der Metalle Eisen Kupfer und Nickel. *Z. Physik.* 36, 913-939.
- [33] Mandel, J. 1966. Contribution theorique a l'etude de l'ecrouissage et des lois de l'écoulement plastique, *Proc. 11th Int. Congr. Appl. Mech. (Munich 1964)*, pp. 502-509, Springer-Verlag.
- [34] Matsuoka, H, Nakai, T., 1977. Stress-strain relationship of soil based on the "SMP". *Proc. Specialty Session 9, IX ICSMFE, Tokyo*, 153-162.

- [35] Mollica, F. and Srinivasa, A.R. 2002. A general framework for generating convex yield surfaces for anisotropic metals. *Acta mater.* 154, 61-84.
- [36] Naghdi, P.M., Essenburg, F. and Koff, W. 1958. An experimental study of initial and subsequent yield surfaces in plasticity. *J. Appl. Mech.* 25, 201-209.
- [37] Naghdi, P.M. and Srinivasa, A.R., 1994. Some general results in the theory of crystallographic slip. *Z. Angew. Math. Phys.* 45, 687-732.
- [38] Menétrey, Ph., Willam, K.J., 1995. Triaxial failure criterion for concrete and its generalization. *ACI Structural Journal* 92, 311-318.
- [39] Newman, K., Newman, J.B., 1971. Failure theories and design criteria for plain concrete. In: *Structure, Solid Mechanics and Engineering Design, Proc. 1969 Southampton Civil Engineering Conf.*, Te'eni, M. Ed., Wiley Interscience, New York, pp. 963-995.
- [40] Ol'khovik, O., 1983. Apparatus for testing of strength of polymers in a three-dimensional stressed state. *Mech. Compos. Mater.* 19, 270-275.
- [41] Ottosen, N.S., 1977. A failure criterion for concrete. *J. Eng. Mech. Div.-ASCE* 103, 527-535.
- [42] Paul, B., 1968. Macroscopic criteria for plastic flow and brittle fracture. In: *Fracture, an advanced treatise*, Liebowitz, H. Ed., Vol. I, pp. 313-496, Academic Press, New York.
- [43] Phillips, A., 1974. Experimental plasticity. Some thoughts on its present status and possible future trends. In: *Symposium on the foundations of plasticity (Warsaw, 1972)*, Sawczuk, A.A. Ed., pp. 193-233, Nordhoff International Publishing, Leyden.
- [44] Roberts, A.W., Varberg, D.E., 1973. *Convex functions*. Academic Press, New York.
- [45] Roscoe, K.H., Burland, J.B., 1968. On the generalized stress-strain behaviour of 'wet' clay, *Engineering Plasticity*, Heyman, J. and Leckie, F.A., Eds., Cambridge University Press, Cambridge.
- [46] Roscoe, K.H., Schofield, A.N., 1963. Mechanical behaviour of an idealised 'wet' clay. *Proc. European Conf. on Soil Mechanics and Foundation Engineering*, Wiesbaden (Essen: Deutsche Gesellschaft für Erd- und Grundbau e. V.), vol. 1, pp. 47-54.
- [47] Rudnicki, J.W. and Rice, J.R. 1975. Conditions for the localization of deformations in pressure-sensitive dilatant materials. *J. Mech. Phys. Solids* 23, 371-394.
- [48] Salençon, J., 1974. *Applications of the theory of plasticity in soil mechanics*. Wiley & Sons, Chichester.
- [49] Schofield, A.N., Wroth, C.P., 1968. *Critical state soil mechanics*, McGraw-Hill Book Company, London.
- [50] Sfer, D., Carol, I., Gettu, R., Etse, G., 2002. Study of the behaviour of concrete under triaxial compression. *ASCE J. Engng. Mech.* 128, 156-163.

- [51] Shield, R.T. 1955. On Coulomb's law of failure in soils. *J. Mech. Phys. Solids* 4, 10-16.
- [52] Sridhar, I., Fleck, N.A., 2000. Yield behaviour of cold compacted composite powders. *Acta mater.* 48, 3341-3352.
- [53] Tasuji, M.E., Slate, F.O., Nilson, A.H., 1978. Stress-strain response and fracture of concrete in biaxial loading. *ACI J.* 75, 306-312.
- [54] Truesdell, C. and Noll, W. 1965. The non-linear field theories of mechanics. In Flügge, S., ed., *Encyclopedia of Physics:III/3*. Springer-Verlag, Berlin.
- [55] Tvergaard, V., 1981. Influence of voids on shear band instabilities under plane strain conditions. *Int. J. Fracture* 17, 389-407.
- [56] Tvergaard, V., 1982. On localization in ductile materials containing spherical voids. *Int. J. Fracture* 18, 237-252.
- [57] Willam, K.J., Warnke, E.P., 1975. Constitutive model for the triaxial behaviour of concrete. Presented at the seminar on Concrete structures subjected to triaxial stresses, ISMES, Bergamo, 1-30.
- [58] Wood, D.M. 1990. Soil behaviour and critical state soil mechanics. Cambridge University Press.
- [59] Yang, W.H., 1980. A useful theorem for constructing convex yield functions. *J. Appl. Mech.* 47, 301-303.
- [60] Yasufuku, N., Murata, H., Hyodo, M. 1991. Yield characteristics of anisotropically consolidated sand under low and high stress. *Soils and Foundations* 31, 95-109.

APPENDIX A. Values of material parameters employed to fit experimental results in Sec. 3.3

The values of the material parameters of the proposed yield function (6)-(9) employed to model the experimental data reported in Figs. 5-9 and Figs. 11-12 are listed in Table 5 below.

Table 5: Values of material parameters employed to fit experimental results in Figs. 5-9 and Figs. 11-12.

	M	p_c	c	m	α	β	γ
Fig. 5(a)	0.5	0.961 MPa	0	2.6	0.1	0	0.9999
Fig. 5(b)	0.48	—	0	5	0.2	0	0.66
Fig. 6(a)	1.1	—	0	3.2	1.9	—	—
Fig. 6(b)	0.76	—	0	3.4	1.85	—	—
Fig. 6(c)	0.94	—	0	1.8	0.8	—	—
Fig. 6(d)	0.64	—	0	3	1.5	—	—
Fig. 7(a)	0.82	$p_c = 100 f_c$	$c = 0.1 f_c$	2	0.05	—	—
Fig. 7(b)	0.76	$p_c = 100 f_c$	$c = 0.2 f_c$	2	0.026	—	—
Fig. 8(a)	1.18	$p_c = 50 f_c$	$c = 0.04 f_c$	2	0.04	—	—
Fig. 8(b)	0.61	$p_c = 30 f_c$	$c = 0.02 f_c$	2	0.3	—	—
Fig. 9(a)	0.40	1000 MPa	110 MPa	2	0.5	—	—
Fig. 9(b)	0.51	800 MPa	80 MPa	2	0.62	—	—
Fig. 11(a)	—	—	—	—	—	0	0.843
Fig. 11(b)	—	—	—	—	—	0	0.862
Fig. 12(a)	0.78	$p_c/f_c = 5.7$	$c/f_c = 0.3$	2	0.1	0	0.6
Fig. 12(b)	0.86	$p_c/f_c = 3.5 \times 10^7$	$c/f_c = 0.08$	1×10^6	1×-10^8	0.12	0.98

APPENDIX B. Covexity of function (53)

We show that the deviatoric section described by eqn (53) is convex, within the range of parameters reported in Tab. 4. To this purpose, a substitution of eqn (53) into condition (37) yields

$$a \cos^2(3\theta) + b \cos(3\theta) + c \geq 0, \quad \theta \in [0, \pi/3], \quad (\text{B.1})$$

where the coefficients a , b and c are:

$$a = \beta^2 (n^2 - 9), \quad (\text{B.2})$$

$$b = \beta n(1 + \beta)(9 - 2n), \quad (\text{B.3})$$

$$c = n^2(1 + \beta)^2 + 9\beta^2(1 - n). \quad (\text{B.4})$$

Since condition (B.1) is bounded by a parabola, it suffices to analyze the position of its vertex to obtain the values of parameters reported in Tab. 4.